ADVANCED FUNCTIONAL MATERIALS
www.afm-journal.de

A Highly Sensitive Graphene-Organic Hybrid Photodetector with a Piezoelectric Substrate

Wei-Chun Tan, Wei-Heng Shih, and Yang Fang Chen**

To create a sensitive photodetector, the transparent and conductive properties of graphene and the optical and photovoltaic properties of poly(3-hexylthiophene) (P3HT) are combined as a hybrid composite. Based on the inherent nature of the band alignment between graphene and P3HT, the photogenerated holes are able to transfer to the graphene layer and improve the photoresponse to be much better than the traditional layer by layer organic system. Additionally, the graphene is deposited on a piezoelectric $Pb(Zr_{0.2}Ti_{0.8})O_3$ (PZT) substrate, and the photoresponse of such composite photodetectors is found to be ten times larger than on SiO_2 base. It is demonstrated that the electric field of the polarization of piezoelectric substrate helps the spatial separation of photogenerated electrons and holes and promotes the hole doping of graphene to enhance the photoconduction. A detailed investigation of graphene layers, thickness of P3HT and time evolution shows that the composite of graphene and P3HT on PZT can be used as a sensitive photodetector and has potential as an effective solar cell. Moreover, with the replacement of P3HT by a thin layer of bulk heterojunction of polymer and fullerene, the photosensitivity can be further increased by more than one order of magnitude.

1. Introduction

Hybrid composites consisting of multicomponent materials have attracted significant attention both in academic and industrial communities due to their unique properties and multifunctionalities, which cannot be found in single component materials.[1,2] To illustrate this potential, we demonstrate a novel photodetector with high gain based on a rationally designed composite composed of graphene, organic molecules and piezoelectric substrate. It is known that good photodetector performance is crucial for the application of binary switches in imaging techniques, light-wave communication, memory storage, and optoelectronic circuits.[3] The 2D material, graphene, has created a great deal of interest in its fundamental physics and chemistry[4,5] and its applications in transistors, optoelectronics,[6] and photodetection.[7–11] However, due to its zero band-gap property, the absorption efficiency of a single graphene layer is found to be as low as 2.3%.[12] One of the feasible ways to increase the absorption is to couple graphene with other highly absorptive materials. Poly(3-hexylthiophene) (P3HT) is known to have a very high absorption coefficient, which has been widely used in organic optoelectronic devices.[13] Additionally, P3HT possesses several unique properties, such as easy fabrication and low cost. Most importantly, one of the key factors to achieve the highly sensitive photodetector based on P3HT/graphene composite arises from the band alignment between P3HT and graphene, which enables the transfer of photogenerated holes from P3HT to graphene, while keeping the photogenerated electrons in P3HT. The high mobility of holes in graphene allows them to recirculate in graphene before they recombine with electrons trapped in P3HT. Consequently, the photosensitivity can be greatly enhanced. Therefore, the newly developed composite material provides an excellent opportunity for practical application in optoelectronic devices, which is better than the traditional layer by layer organic system.[14]

Meanwhile, piezoelectric materials are widely used in electromechanical applications such as sensors, actuators, and energy harvesters, which convert ambient vibration energy into electricity.[15–17] More recently, it has emerged that piezoelectric substrate can be used to change the transport behavior of charge carriers to create various microelectronic devices. For example, the polarization of piezoelectrics can be used as "gate" voltage to tune the charge transport behavior of graphene field-effect transistors (FETs) for nonvolatile memory.[6] Ferroelectric materials with up and down remnant polarizations have been employed in non-volatile ferroelectric field effect memories as gate dielectrics.[18–21] By replacing the typical gate dielectric SiO_2 with a ferroelectric material of high dielectric constant

W.-C. Tan, Prof. Y. F. Chen
Department of Physics
National Taiwan University
No. 1, Sec. 4, Roosevelt Road, Taipei 106
Taiwan, Republic of China
E-mail: yfchen@phys.ntu.edu.tw
W.-C. Tan, Prof. Y. F. Chen
Center for Emerging Material and Advanced Devices
National Taiwan University
No. 1, Sec. 4, Roosevelt Road, Taipei 106, Taiwan, Republic of China
Prof. W.-H. Shih
Department of Materials Science and Engineering
Drexel University
Philadelphia, PA 19104, USA
E-mail: shihwh@drexel.edu

DOI: 10.1002/adfm.201401421

© 2014 WILEY-VCH Verlag GmbH & Co. KGaA, Weinheim

such as lead zirconate titanate (PZT), the transconductance of a FET can be increased. For example, Hong et al. reported a tenfold increase of carrier mobility in few-layer graphene (FLG) FETs when the SiO_2 substrate is replaced by single-crystalline epitaxial $Pb(Zr_{0.2}Ti_{0.8})O_3$ (PZT).[22]

In the past few years, by depositing graphene on a PZT layer, we developed a graphene-PZT FET and demonstrated its optothermal effect.[23] The drain current of graphene-PZT FET can be modulated by an optothermal gating mechanism where PZT served as the gate dielectric and graphene as the drain conductor. The ultrathin graphene layer was deposited by chemical vapor deposition (CVD) and was subsequently transferred to the PZT substrate. An infrared (IR) laser of 1064 nm wavelength and 320 mW power was used as a light source. It was shown that the drain current can be modulated by the incidence of the IR light via the pyroelectric effect of the PZT. Furthermore the drain current could be increased or decreased by the incident IR light by properly orienting the polarization of the PZT layer. The drain current sensitivity of the optothermal FET can reach up to 360 nA mW^{-1} at a drain field of 6.7 kV m^{-1} more than five orders of magnitude higher than that of the photogating transistors based on carbon nanotube on SiO_2/Si substrate. Graphene is an excellent component for pyroelectric FET due to its high optical transparency and conductance. Similarly, a field-effect transistor using ZnO nanorod instead of graphene on PZT layer was also demonstrated.[24] Inspired by our previous work, in this paper we further examine the effect of a piezoelectric substrate on the enhancement of photoresponse of a P3HT/graphene composite to achieve highly sensitive photodetectors. However, in contrast to earlier studies, the laser power used in this study is less than 10 mW, which does not change the polarization of the PZT and does not involve the pyroelectric effect of PZT.

2. Results and Discussion

The fabricated photodetector on SiO_2 substrate which shows the structure in **Figure 1** was characterized using current–voltage measurements under illumination with a 325 nm laser. In order to understand the behavior of this device, we examined the mechanism of the charge transfer between graphene and P3HT. From **Figure 2**a, the transport behaviors (drain current I_d vs. gate voltage V_g) were recorded when P3HT was coated on graphene transistor. P3HT is a p-type organic semiconductor and is a well-known hole transporting material due to the higher transfer rate of holes than that of electrons.[25] It is shown that after P3HT coating, the Dirac point shifts to a negative gate voltage indicating an n-type doping in graphene film.[26] Because of this shift, we know that the Fermi level of the current intrinsic CVD graphene is lower than that of P3HT, which is consistent with the estimated work functions given in previous reports.[27] Therefore, we expect the holes in graphene will transfer to P3HT after coating and induce a built-in electric field to equilibrate the Fermi level.

Furthermore, when comparing the transport behavior in the dark condition to that after 325 nm laser exposure as shown in Figure 2a, one can see the Dirac point shifts to the opposite direction. This phenomenon is caused by electron-hole pairs

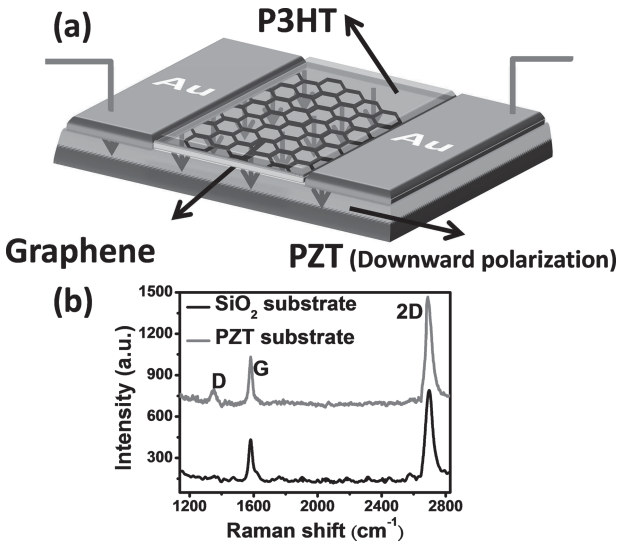

Figure 1. a) Schematic view of the experimental device setup. b) Micro-Raman spectrum for graphene on the SiO_2 and PZT substrates with indication of graphene Raman peaks.

generated in P3HT film by the 325 nm laser. Under light exposure, the holes from P3HT are transferred to graphene to bring about the p-type doping behavior according to the band bending formed by the built-in field. That is the reason why the conductance increases under illumination.[26] As shown in Figure 2b, n-type doping effect of P3HT in graphene increases the concentration of hole carriers in P3HT resulting in more positive charge than electrons in P3HT. Consequently, the mobility of holes transport to graphene is higher than electrons by the corresponding build-in field. This leads to electrons trapped in P3HT as well as holes transport to graphene resulting in higher photoresponse R_{ph} which was given by[2,28]

$$R_{ph} = \frac{\Delta I(A)}{P(W)} \tag{1}$$

where ΔI is the photocurrent and P is the laser power. Therefore, coating P3HT on graphene can enhance photosensitive behavior of graphene.

On the other hand, the graphene without P3HT behaves in an opposite manner to that coated with P3HT. As shown in Figure 2c, the photoresponse is hardly seen in graphene without P3HT. Note that it required much higher laser power (mW) to see any effect without P3HT compared to the micro-Watt laser used in the case with P3HT (Figure 2b). The small current decrease caused by the laser beam on graphene is speculated to be due to gas molecular desorption as shown in previous study in the literature.[29] Because of the low optical absorption of graphene, the photoresponse is relatively small. In contrast, Figure 2b showed the photoresponse of graphene with P3HT is due to hole doping which increases the charge carrier density in the graphene film.

To improve the performance, we fabricated the composite photodetector on PZT substrate with downward polarization. As shown in **Figure 3**a, the photoresponse of photodetector is much enhanced by the PZT substrate. It can be seen that

© 2014 WILEY-VCH Verlag GmbH & Co. KGaA, Weinheim

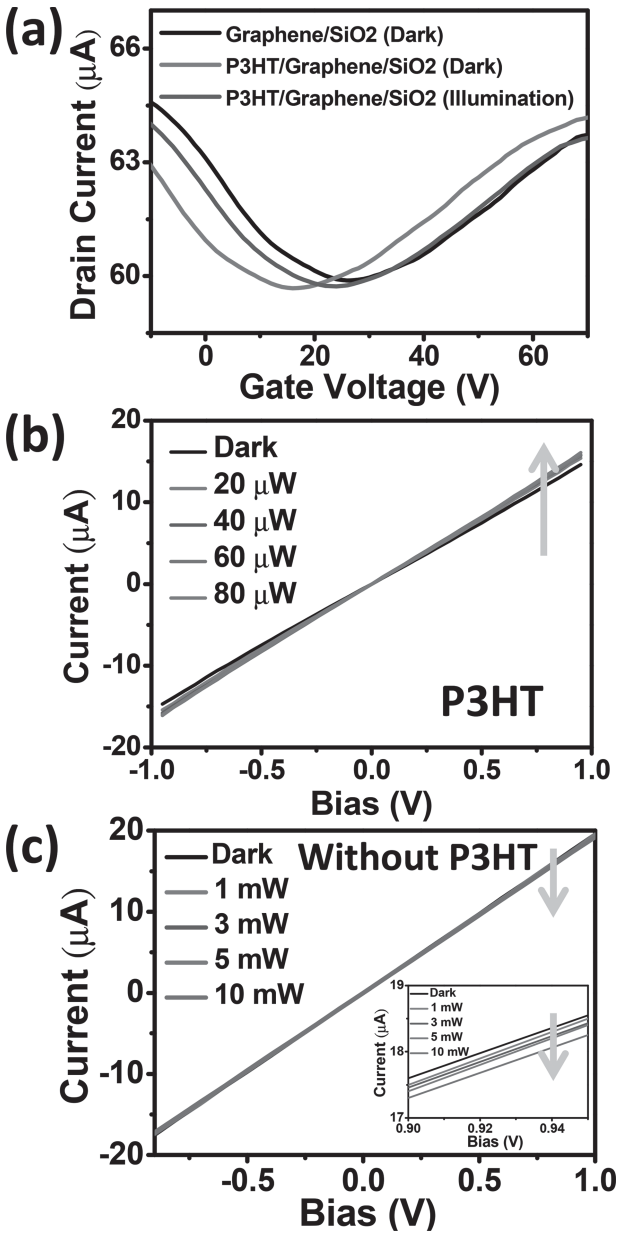

Figure 2. a) Drain current at V_{ds} = 1 V as a function of gate voltage for different devices on SiO_2 substrate. b) Photoresponse of P3HT/graphene and c) graphene without P3HT under different laser powers as a function of drain-source voltage on SiO_2 substrate. Inset: an expanded region of the plot shown in (c).

the conductance increased by 200% upon laser illumination. In contrast, the conductance increased only about 20% on SiO_2 substrate (Figure 2b) which shows the PZT substrate can enhance the photoresponse of the detector up to ten times compared to SiO_2 substrate.

The shift of Dirac point by the P3HT coating on graphene on SiO_2 shown in Figure 2a is now much larger for P3HT coating on graphene on PZT substrate with downward polarization. This is clearly seen in Figure 3b with the substantial Dirac point shifts. In addition, as shown in Figure 3c, when exposed to varying degree of laser power, the Dirac point shifts to more positive voltage. In the case of PZT substrate, the shift of Dirac point is larger than that on SiO_2 substrate shown in Figure 2a. We can see that the Dirac shift is correlated to the laser power. As the light power increases, the hole quasi-Fermi level increases, as summarized in Figure 3d. It also shows the Dirac shift of graphene on different substrates. It can be seen that the substrate with downward polarization has the largest shift and the upward polarization has the smallest while SiO_2 substrate has the intermediate shift. We can also utilize this result to obtain the Fermi level shift of graphene correlated to the laser power as shown in the Figure S1 (Supporting Information). The PZT substrate shows two times more shift than the SiO_2. To understand the behavior in Figure 3d, we first note that there are bound charges on the surfaces of PZT. At the top surface of a PZT with downward polarization there were bound negative charges. On the other hand, upward polarization would have positive charges bound on the top surface. When the graphene was transferred to PZT substrate with downward polarization, the graphene was in contact with the bound negative charges on the PZT surface. Although the charges will not transfer and dope the graphene, they would attract hole carriers toward graphene layer thus increasing the hole quasi-Fermi level.[23] Because of this effect by PZT, graphene on downward polarization PZT will have lower Fermi level than the graphene on SiO_2 that can be seen in Figure 2a and Figure 3b. Figure 3e illustrates the effect of light exposure and the PZT substrate using the schematic energy level diagram. Without PZT substrate, the n-type doping of P3HT on graphene creates a built-in electric field attracting the photogenerated holes from P3HT under light exposure. With PZT substrate of downward polarization (D-PZT), the permanent surface dipoles in the substrate provides electric field to modify the charge carrier concentration in the graphene and enhances the band bending level between graphene and P3HT thereby having higher photoresponse and Dirac point shift. On the other hand, the upward polarization PZT would raise Fermi level of graphene and decrease the band bending level to the level lower than on SiO_2 substrate. That is why we observe very small Dirac point shift on upward polarization PZT substrate.

To further examine the mechanism of bound-charge induced carriers concentration in graphene, we studied the measurement with different number of graphene layers as shown in **Figure 4**a. The increasing number of graphene layers is confirmed by the Raman spectrum (shown in the inset) which is consistent with that shown in the literature.[30] It was found that the photoresponse of the photodetector varied with the number of layers. Monolayer graphene on downward polarization PZT substrate has a larger photoresponse than on SiO_2. When increasing the number of graphene layers, the photoresponse decayed significantly on PZT but only slightly on SiO_2 that was due to the small mobility decrease from monolayer to multilayer graphene.[31] The decrease in photoresponse is due to the increasing number of graphene layers screening the electric field from the bound charges of PZT. As reported previously,[32] monolayer graphene has small screening effect than bulk metal electrode. When we increased the number of layers, multilayer graphene could be thought of as a bulk metal which screens the bound charges from PZT. Besides the results in Figure 3d, the results in Figure 4a verify that the polarization of the PZT

© 2014 WILEY-VCH Verlag GmbH & Co. KGaA, Weinheim

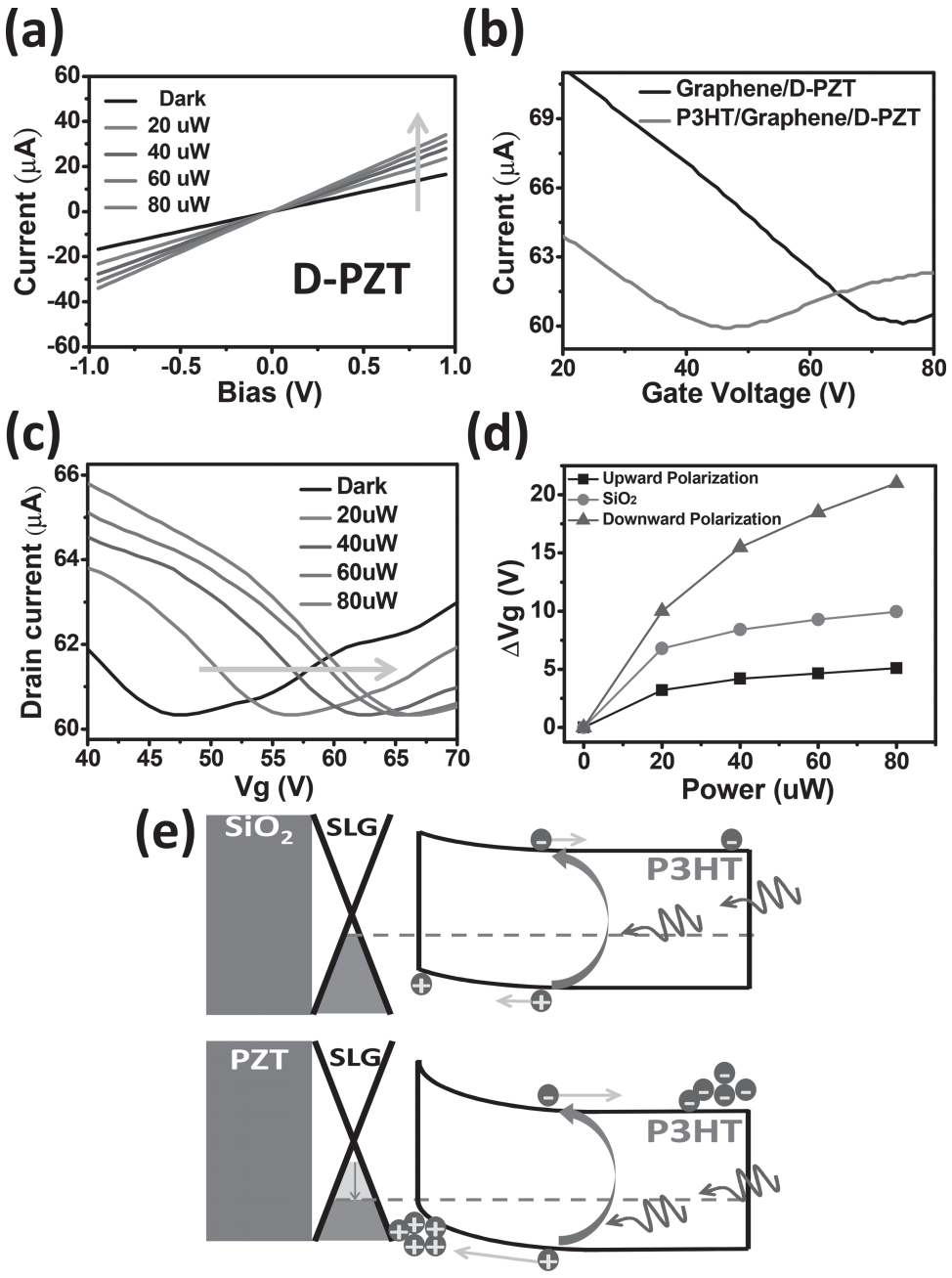

Figure 3. a) Photoresponse of P3HT/graphene composite under different laser powers as a function of drain-source voltage on downward polarization PZT (D-PZT) substrate. b) Drain current at V_{ds} = 1 V as a function of gate voltage for graphene and P3HT/graphene devices on D-PZT substrate. c) Drain current at V_{ds} = 1 V as a function of gate voltage for P3HT/graphene on D-PZT substrate under different 325 nm laser powers. d) Dirac point shift of different substrates vs. laser power. e) Energy level diagram of the P3HT/graphene/PZT interface: lower Fermi level of graphene creates higher build-in field by D-PZT than SiO_2 substrate.

substrate plays a key role on the photoresponse of graphene. Because of this reason, the single atom thick 2D graphene is a very good material to combine with PZT substrate. If we can pattern graphene to be porous, it can also reduce its screening effect and enhance the photoresponse.[33,34]

We also increase the P3HT film thickness under the same light irradiation on polarization and non-polarization substrate and study its behavior. Although P3HT is widely used in organic solar cell by its high absorption in visible spectrum and affordable material as hole transport layer,[13] its intrinsic properties of low mobility and short lifetime limits its application as photodetector. In general, the photoresponse was found to depend on the amount of semiconductor and tend to saturate with increasing thickness.[35] By increasing the thickness of P3HT in Figure 4b, we found there is a maximum photoresponse thickness of P3HT on PZT and SiO_2 substrate, respectively. Although increasing the amount of P3HT can increase the number of hole carriers in graphene, too thick P3HT is not

© 2014 WILEY-VCH Verlag GmbH & Co. KGaA, Weinheim

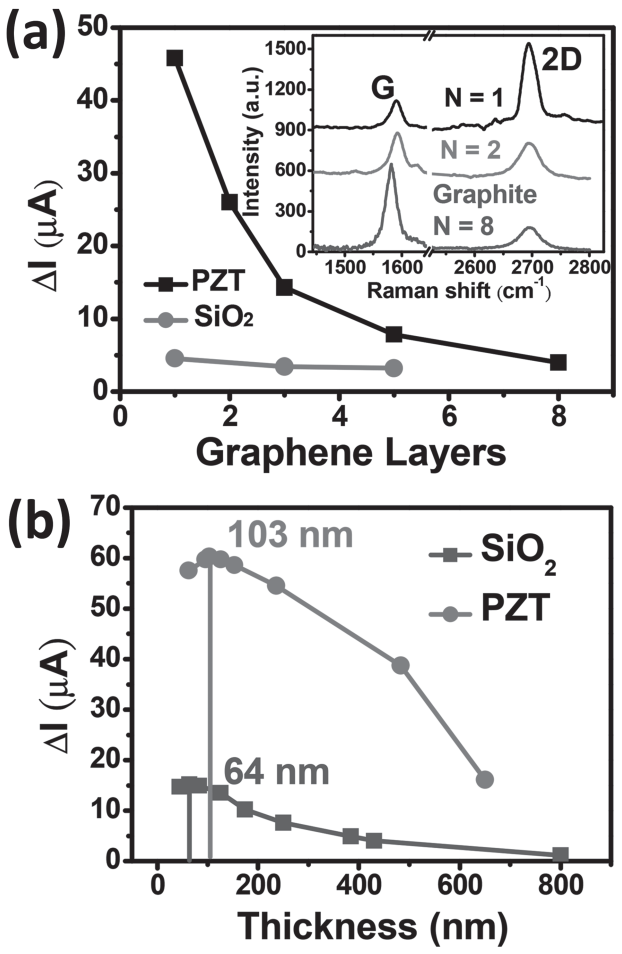

Figure 4. a) Degree of photoresponse vs. different number of graphene layers with about 200 nm thickness of P3HT. Inset: The micro-Raman spectrum for different layers of graphene on PZT substrates. b) Photoresponse vs. thickness of P3HT on SiO_2 and PZT substrates.

favorable because some of the excitons generated in very thick P3HT film would exceed the diffusion length and will recombine before they are transported to graphene. As a result, the photoresponse would decay when the thickness of P3HT is larger than the thickness corresponding to the maximum photoresponse. Comparing the result in Figure 4b, we can see that the photodetector has not only much higher photoresponse but also larger thickness of maximum photoresponse on downward polarization PZT substrate than SiO_2. It shows the PZT substrate could increase the effective transport distance from 64 nm to 103 nm by bound charges. The average effective transport distance increase also implies the drift velocity of hole in P3HT can be improved by the electric field from PZT substrate which is given generally by: $v = \mu E$[36] where v is the drift velocity, μ is the mobility, and E is the effective build-in field which came from the band bending. This result is consistent with the previous result[24] and shows that the PZT substrate can induce the photodetector to a higher sensitivity.

The kinetic behavior of the photoresponse is also studied and the results on different substrate are shown in **Figure 5**a. In order to obtain systematic data, we monitored the change of photocurrent rather than the photocurrent itself for comparison. It is observed that there is a clear enhancement of photoresponse on PZT substrate with downward polarization than that on SiO_2 substrate due to the bound charge inducing band bending. Meanwhile, the photoresponse on PZT with upward polarization shows the opposite effect of reducing photoresponse. From many phototransistors reported in the literature, the current increase with time under illumination can be fitted with a series of two exponential functions:[37]

$$\Delta I = \Delta I_1\left[1-\exp\left(-\frac{1}{\tau_1}\right)\right]+\Delta I_2\left[1-\exp\left(-\frac{1}{\tau_2}\right)\right] \quad (2)$$

Here τ_1 and τ_2 are the time constants that corresponds to the hole transfer from P3HT to graphene and the charge transfer in P3HT film respectively. As shown in Figure 5b, the experimental data can be fitted by the equation nicely. Using the data in Figure 5a, τ_1 and τ_2 can be extracted according to Equation (2) and all of the fitting results are shown in **Table 1**. The value of τ_1 and τ_2 for the device without any polarization are 0.35 s and 4.02 s which agreed well with reported results of phototransistor charge exchange in hybrid semiconductor with graphene.[35] When the substrate of photodetector is PZT with downward polarization, the current increases more rapidly compared to that of SiO_2 substrate. Moreover, the time constants are shorter with τ_1 and τ_2 of (0.18 s) and (1.62 s) respectively. This is expected because the stronger band bending caused by PZT induced a higher build-in field which accelerated the charge transfer. Thus, under the help of PZT substrate, the photodetector can respond faster. Meanwhile, the device on PZT with upward polarization showed smaller and slower photoresponse. Its longer time constants in Table 1 are expected because of the polarization bound charge decreases the band bending level which impeded the holes transfer to graphene. After switching off the illumination, the current dropped off as shown in Figure 5a which is due to the recombination of the accumulated electrons with holes in P3HT. The time evolution during light off can be fitted by Equation (3):

$$\Delta I = \Delta I_3 \exp\left(-\frac{1}{\tau_3}\right)+\Delta I_4 \exp\left(-\frac{1}{\tau_4}\right) \quad (3)$$

and is shown in the inset of Figure 5b. Comparing these results of time constants of three different substrates in Table 1, we find that PZT substrate with downward polarization has the longest time constants. This result can be understood because the negative bound charge from the substrate maintains the band bending potential barrier, which keeps electrons trapped in P3HT and separate them from the holes that are transferred to graphene. As the band bending is increased by PZT, the probability of electron recombination is decreased and the photoresponse decay rate also decreased. In contrast, the substrate with the opposite polarization gives a rapid decay of photocurrent. In other words, using a PZT with downward polarization as substrate can extend the time lapse of photoresponse signal and amplify the strength of signal. It has the potential to be used for light memory for weak signal storage.[38,39]

As the previous work reported,[23] light can change the polarization of PZT through the pyroelectric effect because of

© 2014 WILEY-VCH Verlag GmbH & Co. KGaA, Weinheim

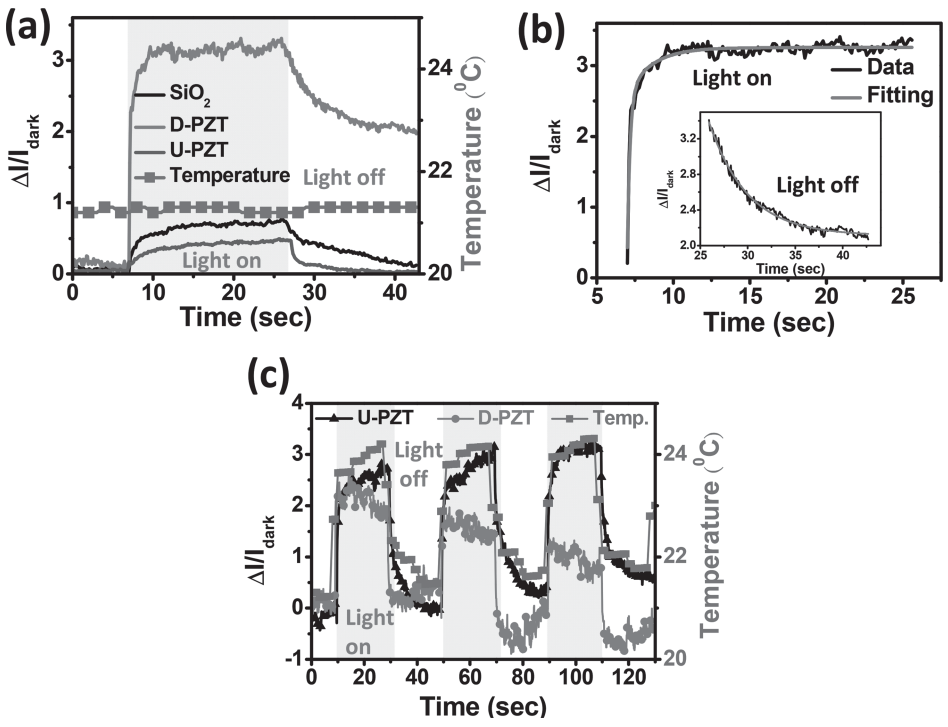

Figure 5. a) Extraction of photoresponse of different substrates during the illumination light-on and light-off with the corresponding temperature evolution under the illumination of 325 nm laser power of about a) 100 μW and c) 100 mW. b) The light-on curve fitting from panel (a) (downward polarization PZT) by Equation (1); the inset is the light-off curve fitting by Equation (2).

temperature change. This optothermal field effect was demonstrated by using high power laser of 100 mW. In contrast, the current experiments used laser power of less than 10 mW which does not change the polarization of the PZT because the temperature of the system remains almost constant as shown in Figure 5a with temperature change less than 0.2 °C. In addition, the photoresponse is much higher than that from optothermal indicating the response mostly came from the enhancement due to the polarization bound charge. To further check the PZT substrate behavior, Figure 5c shows the time evolution of P3HT/graphene phototransistor device under high laser power of ≈100 mW. It can be seen that the temperature varied significantly due to the illumination. Due to the pyroelctric effect of PZT, the degree of polarization would decrease by increasing temperature. As a result, the photoresponses of downward and upward PZTs are found to be similar with the SiO_2 substrate when high power laser was used. It can also be noted in Figure 5c that with the passing of time, the average current of each device settled toward a small value indicating the temperature evolution of the photodetector. For example, the average current for the device with downward polarization decreased because of the high power laser increased the temperature and reduced the bound charge thus suppressing the holes doping level in graphene. This phenomenon would reduce the photoresponse of this device and is consistent with the results reported previously.[23,24] To further promote the photosensitivity of the device, the P3HT material was replaced by the mixture of P3HT and PCBM, which has been frequently used in organic solar cells.[13] It is known the bulk heterojunctions of P3HT and (6,6)-phenyl-C_{61}-butyric acid methyl ester (PCBM) can efficiently enhance the separation of photogenerated electrons and holes. For example, **Figure 6**a shows the much higher photoresponse when mixing the PCBM in P3HT with a weight ratio of 1:1 to fabricate a P3HT:PCBM structure on graphene. Clearly there is a good potential for this to develop into an efficient solar cell and we will study this in a future publication.

Table 1. The time constant extracted from Figure 5a using Equation (1) and Equation (2).

	D-PZT	U-PZT	SiO_2
τ_1(s)	0.182	1.541	0.347
τ_2(s)	1.624	13.683	4.025
τ_3(s)	4.069	0.557	0.725
τ_4(s)	13.192	6.007	9.843

To compare the results, Figure 6b shows the gain of the different composites. The photocurrent gain (Γ) was calculated by the following expression:[2]

$$\Gamma = \frac{\Delta i / q}{P / h\upsilon} \frac{1}{\eta} \tag{4}$$

where Δi is the current difference between light illumination and dark condition, q is the electron charge, $h\upsilon$ is the photon energy of incident light and P is the incident power. Finally, η is the efficiency of the photon absorption to generate electron-hole pairs which is dominated by quantum efficiency correlation with the absorption coefficient of P3HT and P3HT:PCBM. In this approach, we set η to be unity for the purpose of comparison. From Figure 6b, we can clearly see the photocurrent gain with PZT substrate is ten times higher than with SiO_2. By replacing the P3HT with P3HT:PCBM, we can further enhance the gain to about 10^3. This result shows that using PZT substrate can create a highly sensitive organic-containing photodetector that is better than the traditional layer by layer organic system.[14]

3. Conclusion

We have demonstrated that the composite consisting of graphene and P3HT can be used to create a highly sensitive

© 2014 WILEY-VCH Verlag GmbH & Co. KGaA, Weinheim

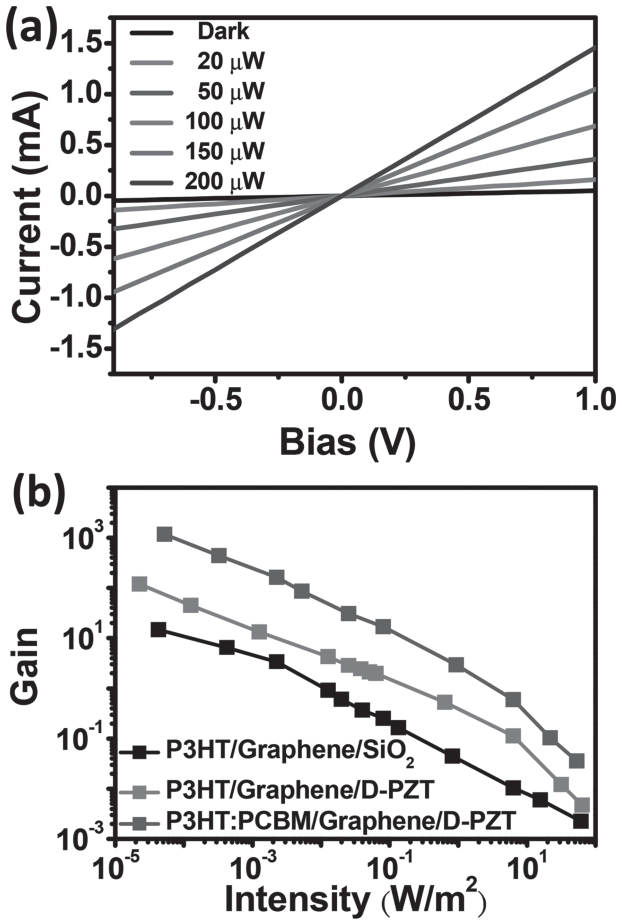

Figure 6. a) Photoresponse of P3HT:PCBM/graphene composite under different laser powers on downward polarization PZT (D-PZT) substrate. b) The photocurrent gain comparison between the three different conditions.

photodetector with easy fabrication and low cost for practical applications. The underlying mechanism arises from the suitable band alignment between graphene and P3HT, which causes the transfer of photogenerated holes from P3HT to graphene and greatly enhances the photoresponse. Furthermore, we show that the PZT substrate can have an important effect on the P3HT/graphene photodetector on top of it due to its bound change and create a significant improvement on the photoresponse of the hybrid composite. It provides an excellent opportunity to enhance the photoresponse without external power consumption that is also very useful and economical. The newly designed organic/graphene/PZT photodetector has high gain and has potential for highly efficient solar cells, which may open up an excellent alternative route for the creation of next generation optoelectronic devices.

4. Experimental Section

Device Fabrication: To fabricate a graphene-based organic photodetector on PZT substrate as shown in Figure 1a, the graphene was grown on a copper foil in vacuum via CVD (chemical vapor deposition) method.[40] After passing methane and hydrogen gases in a tube furnace at 1000 °C for 2 h, the graphene samples were transferred to PZT (T105-A4E-602, Piezo Systems, Boston, MA) substrate and silicon chip with 300 nm SiO_2 respectively. To obtain systematic data, graphene deposited on the same copper foil was used. The PZT layers used in this experiment were 127 μm and the polarization had been poled to the direction perpendicular to the surface with top and bottom Ni electrodes which were later removed by HNO_3 solution after poling. The graphene transferring process to PZT is carried out through polymethyl methacrylate (PMMA) coating as a template and iron (III) nitrate solution to remove copper foil.[30] After that, the as-grown PMMA/graphene was transferred onto the PZT. To avoid damaging the graphene due to the roughness of PZT, the transferred samples were placed in a petri dish with boiling acetone vapor to etch the PMMA. The characteristics and quality of the graphene grown on SiO_2 or PZT substrate are characterized by Raman spectroscopy (Jobin Yvon T64000) and the results are shown in Figure 1b.[41] A copper mesh of 12 μm wide was then used to define the contact pattern to create Ti/Au (30/300nm) electrodes by e-gun thermal vapor deposition. Finally, 20 mg of pure P3HT poly(3-hexythiophene) (Lumtech, Taiwan) and mixture of P3HT (20 mg) and (6,6)-phenyl C_{61} butyric acid methyl ester (20 mg) (P3HT:PCBM) (Lumtech, Taiwan) were dissolved in 1 mL o-dichlorobenzene forming P3HT and P3HT:PCBM solution then spin coating on graphene/PZT substrate respectively with different rotation speeds.

To demonstrate the effect of the PZT substrate, we transferred three pieces of graphene which were deposited on the same copper foil to the SiO_2 layer, upward and downward polarization PZT substrate, respectively. First, the devices were placed in a chamber and with the help of a vacuum pump the pressure was controlled at 50 mTorr. Second, the temperature was increased step by step and measured the corresponding graphene dark current of the three devices under the bias of 1 V. When the temperature reached around 150 °C, the currents became almost the same. In Figure S2 (Supporting Information), it is shown that the high temperature above 150 °C erased the polarization of PZT confirming the existence of PZT polarization effect at room temperature. The currents of the three devices above 150 °C were slightly different results from the differences in surface state and graphene-substrate interaction. This experiment clearly demonstrated the influence of polarization of the PZT substrate.

To evaluate the stability of the photodetector against temperature, the device was heated to a goal temperature (G.T.), held for 10 min and then cooled down to the room temperature (R.T.) of about 20 °C. From the Figure S3 (Supporting Information), it was observed that the polarization of this device remained at 70% of the original value when heated to 120 °C. When the PZT was treated at higher than 160°C, which was near the poling temperature, the polarization decreased steeply and could not recover. Based on the above experimental observations, the photodetectors have sufficient stability at room temperature.

Supporting Information

Supporting Information is available from the Wiley Online Library or from the author.

Acknowledgements

This work was supported by the National Science Council and Ministry of Education of the Republic of China.

Received: May 1, 2014
Revised: July 4, 2014
Published online: September 8, 2014

[1] B. M. Novak, *Adv. Mater.* **1993**, *5*, 422.
[2] M. L. Lu, C. W. Lai, H. J. Pan, C. T. Chen, P. T. Chou, Y. F. Chen, *Nano Lett.* **2013**, *13*, 1920.

© 2014 WILEY-VCH Verlag GmbH & Co. KGaA, Weinheim

[3] T. Y. Zhai, L. Li, Y. Ma, M. Y. Liao, X. Wang, X. S. Fang, J. N. Yao, Y. Bando, D. Golberg, *Chem. Soc. Rev.* **2011**, *40*, 2986.
[4] S. Shivaraman, R. A. Barton, X. Yu, J. Alden, L. Herman, M. V. S. Chandrashekhar, J. Park, P. L. McEuen, J. M. Parpia, H. G. Craighead, M. G. Spencer, *Nano Lett.* **2009**, *9*, 3100.
[5] T. O. Wehling, K. S. Novoselov, S. V. Morozov, E. E. Vdovin, M. I. Katsnelson, A. K. Geim, A. I. Lichtenstein, *Nano Lett.* **2008**, *8*, 173.
[6] F. Bonaccorso, Z. Sun, T. Hasan, A. C. Ferrari, *Nat. Photonics* **2010**, *4*, 611.
[7] J. Park, Y. H. Ahn, C. Ruiz-Vargas, *Nano Lett.* **2009**, *9*, 1742.
[8] E. J. H. Lee, K. Balasubramanian, R. T. Weitz, M. Burghard, K. Kern, *Nat. Nanotechnol.* **2008**, *3*, 486.
[9] F. N. Xia, T. Mueller, R. Golizadeh-Mojarad, M. Freitag, Y. M. Lin, J. Tsang, V. Perebeinos, P. Avouris, *Nano Lett.* **2009**, *9*, 1039.
[10] F. N. Xia, T. Mueller, Y. M. Lin, A. Valdes-Garcia, P. Avouris, *Nat. Nanotechnol.* **2009**, *4*, 839.
[11] T. Mueller, F. N. A. Xia, P. Avouris, *Nat. Photonics* **2010**, *4*, 297.
[12] R. R. Nair, P. Blake, A. N. Grigorenko, K. S. Novoselov, T. J. Booth, T. Stauber, N. M. R. Peres, A. K. Geim, *Science* **2008**, *320*, 1308.
[13] J. Y. Chen, F. C. Hsu, Y. M. Sung, Y. F. Chen, *J. Mater. Chem.* **2012**, *22*, 15726.
[14] X. Gong, M. H. Tong, Y. J. Xia, W. Z. Cai, J. S. Moon, Y. Cao, G. Yu, C. L. Shieh, B. Nilsson, A. J. Heeger, *Science* **2009**, *325*, 1665.
[15] Z. L. Wang, J. H. Song, *Science* **2006**, *312*, 242.
[16] X. D. Wang, J. Zhou, J. H. Song, J. Liu, N. S. Xu, Z. L. Wang, *Nano Lett.* **2006**, *6*, 2768.
[17] F. Gattringer, M. Nader, M. Krommer, H. Irschik, *J. Vib. Control* **2003**, *9*, 965.
[18] Y. Zheng, G. X. Ni, C. T. Toh, C. Y. Tan, K. Yao, B. Ozyilmaz, *Phys. Rev. Lett.* **2010**, *105*, 166602.
[19] J. Hoffman, X. A. Pan, J. W. Reiner, F. J. Walker, J. P. Han, C. H. Ahn, T. P. Ma, *Adv. Mater.* **2010**, *22*, 2957.
[20] L. Liao, H. J. Fan, B. Yan, Z. Zhang, L. L. Chen, B. S. Li, G. Z. Xing, Z. X. Shen, T. Wu, X. W. Sun, J. Wang, T. Yu, *ACS Nano* **2009**, *3*, 700.
[21] X. Hong, J. Hoffman, A. Posadas, K. Zou, C. H. Ahn, J. Zhu, *Appl. Phys. Lett.* **2010**, *97*, 033114.
[22] X. Hong, A. Posadas, K. Zou, C. H. Ahn, J. Zhu, *Phys. Rev. Lett.* **2009**, *102*, 136808.
[23] C. Y. Hsieh, Y. T. Chen, W. J. Tan, Y. F. Chen, W. Y. Shih, W. H. Shih, *Appl. Phys. Lett.* **2012**, *100*, 113507.
[24] C. Y. Hsieh, M. L. Lu, J. Y. Chen, Y. T. Chen, Y. F. Chen, W. Y. Shih, W. H. Shih, *Nanotechnology* **2012**, *23*, 355201.
[25] V. Shrotriya, J. Ouyang, R. J. Tseng, G. Li, Y. Yang, *Chem. Phys. Lett.* **2005**, *411*, 138.
[26] G. Konstantatos, M. Badioli, L. Gaudreau, J. Osmond, M. Bernechea, F. P. G. de Arquer, F. Gatti, F. H. L. Koppens, *Nat. Nanotechnol.* **2012**, *7*, 363.
[27] Y. M. Sung, F. C. Hsu, D. Y. Wang, I. S. Wang, C. C. Chen, H. C. Liao, W. F. Su, Y. F. Chen, *J. Mater. Chem.* **2011**, *21*, 17462.
[28] S. H. Cheng, T. M. Weng, M. L. Lu, W. C. Tan, J. Y. Chen, Y. F. Chen, *Sci Rep* **2013**, *3*, 2694.
[29] Y. M. Shi, W. J. Fang, K. K. Zhang, W. J. Zhang, L. J. Li, *Small* **2009**, *5*, 2005.
[30] A. Reina, X. T. Jia, J. Ho, D. Nezich, H. B. Son, V. Bulovic, M. S. Dresselhaus, J. Kong, *Nano Lett.* **2009**, *9*, 30.
[31] K. Nagashio, T. Nishimura, K. Kita, A. Toriumi, *Appl. Phys. Express* **2009**, *2*, 025003.
[32] L. Britnell, R. V. Gorbachev, R. Jalil, B. D. Belle, F. Schedin, A. Mishchenko, T. Georgiou, M. I. Katsnelson, L. Eaves, S. V. Morozov, N. M. R. Peres, J. Leist, A. K. Geim, K. S. Novoselov, L. A. Ponomarenko, *Science* **2012**, *335*, 947.
[33] B. Liu, M. A. McCarthy, Y. Yoon, D. Y. Kim, Z. C. Wu, F. So, P. H. Holloway, J. R. Reynolds, J. Guo, A. G. Rinzler, *Adv. Mater.* **2008**, *20*, 3605.
[34] M. G. Lemaitre, E. P. Donoghue, M. A. McCarthy, B. Liu, S. Tongay, B. Gila, P. Kumar, R. K. Singh, B. R. Appleton, A. G. Rinzler, *ACS Nano* **2012**, *6*, 9095.
[35] Z. H. Sun, Z. K. Liu, J. H. Li, G. A. Tai, S. P. Lau, F. Yan, *Adv. Mater.* **2012**, *24*, 5878.
[36] D. M. Caughey, R. E. Thomas, *Proc. Inst. Electrical Electron. Eng.* **1967**, *55*, 2192.
[37] B. Chitara, L. S. Panchakarla, S. B. Krupanidhi, C. N. R. Rao, *Adv. Mater.* **2011**, *23*, 5339.
[38] R. J. Chen, N. R. Franklin, J. Kong, J. Cao, T. W. Tombler, Y. G. Zhang, H. J. Dai, *Appl. Phys. Lett.* **2001**, *79*, 2258.
[39] C. H. Kim, M. H. Choi, S. H. Lee, J. Jang, S. Kirchmeyer, *Appl. Phys. Lett.* **2010**, *96*, 123301.
[40] X. S. Li, W. W. Cai, J. H. An, S. Kim, J. Nah, D. X. Yang, R. Piner, A. Velamakanni, I. Jung, E. Tutuc, S. K. Banerjee, L. Colombo, R. S. Ruoff, *Science* **2009**, *324*, 1312.
[41] M. S. Dresselhaus, G. Dresselhaus, M. Hofmann, *Philos. Trans. R. Soc. A* **2008**, *366*, 231.

© 2014 WILEY-VCH Verlag GmbH & Co. KGaA, Weinheim